STATISTICAL, NONLINEAR, AND SOFT MATTER PHYSICS

Passive Scalar Transport in Peripheral Regions of Random Flows[1]

A. Chernykh[a,b] and V. Lebedev[c,d]

[a]*Institute of Automation and Electrometry, Siberian Branch of the Russian Academy of Sciences, Novosibirsk, 630090 Russia*
[b]*Novosibirsk State University, Novosibirsk, 630090 Russia*
[c]*Landau Institute for Theoretical Physics, Russian Academy of Sciences, Moscow, 117334 Russia*
[d]*Moscow Institute of Physics and Technology, Moscow, 141700 Russia*
e-mail: chernykh@iae.nsk.su
Received January 13, 2011

Abstract—We investigate statistical properties of the passive scalar mixing in random (turbulent) flows assuming its diffusion to be weak. Then at advanced stages of the passive scalar decay, its unmixed residue is primarily concentrated in a narrow diffusive layer near the wall and its transport to the bulk goes through the peripheral region (laminar sublayer of the flow). We conducted Lagrangian numerical simulations of the process for different space dimensions *d* and revealed structures responsible for the transport, which are passive scalar tongues pulled from the diffusive boundary layer to the bulk. We investigated statistical properties of the passive scalar and of the passive scalar integrated along the wall. Moments of both objects demonstrate scaling behavior outside the diffusive boundary layer. We propose an analytic scheme for the passive scalar statistics, explaining the features observed numerically.

1. INTRODUCTION

Stochastic dynamics of scalar fields such as the temperature or concentration of pollutants in random (turbulent) flows is of great importance in different physical contexts, from cosmology to microfluidics. If the back reaction of the field to the flow is negligible, then the field is called a passive scalar. We consider the passive scalar in random flows, where the flow velocity varies randomly in time. Theoretical examination of dynamical and statistical properties of the passive scalar in random flows goes back to classical works of Obukhov [1] and Corrsin [2], where a phenomenology for the passive scalar statistics in turbulent flows was developed in the spirit of the Kolmogorov scheme [3]. Modern understanding of the passive scalar statistics in turbulent flows is reflected in [4—7] (see also [8—10]). The mixing problem for the passive scalar has also been investigated for chaotic flows [11]. An interesting example of a random flow is the so-called elastic turbulence, discovered in polymer solutions in [12]. Observations of the passive scalar statistics in the elastic turbulence were reported in [13].

In the 1990s, a series of theoretical works devoted to the passive scalar statistics were done in the framework of the so-called Kraichnan model, where the turbulent flow is assumed to be short-correlated in time and to have a definite scaling. Those works revealed general features of the passive scalar statistics in turbulent flows including the so-called anomalous scaling and intermittency [14—16] (see also reviews [17, 18]).

However, the approach implies spacial homogeneity of the flow statistics and is therefore not directly applicable to near-wall regions.

In this paper, we investigate the passive scalar statistics in peripheral regions of a vessel where the developed (high-Reynolds) turbulence is excited. Speaking about the peripheral regions of turbulent flows, we understand a laminar (viscous) sublayer formed near walls where the velocity field can be considered as smooth (it varies over distances of the order of the sublayer thickness). However, the velocity remains a random function of time there. A certain laminar boundary layer is also characteristic of the elastic turbulence [19]. The passive scalar statistics in the peripheral region is determined by a complicated interplay of its diffusion and random advection in the highly anisotropic situation caused by the presence of the walls.

We are interested in advanced stages of the passive scalar decay under the assumption that the Peclet or the Schmidt number is large. In this case, the unmixed fraction of the passive scalar is located mainly in a narrow diffusive layer near the wall, thinner than the thickness of the peripheral region [20]. Then the passive scalar transport to the bulk goes through the peripheral region outside the diffusive layer. Just this peripheral region plays a crucial role in formation of statistical characteristics of the passive scalar transport. The same reasoning can be applied to a stationary case related, e.g., to a permanent heat flow going from the walls through the periphery region to the bulk. Moreover, fast chemical reactions can be analyzed within the same scheme (see [21]). A theoretical

[1] The article is published in the original.

approach to the problem was developed in [22], and principal predictions of the theory were confirmed by experiment in [23].

To check the theoretical predictions in detail, we conducted extensive numerical simulations of the problem based on the Lagrangian dynamics of particles representing the passive scalar. To establish main qualitative properties of the passive scalar transport in the peripheral regions, we focused on the two-dimensional case (2d). However, a great advantage of the Lagrangian scheme is the possibility to extend the approach to higher dimensions without major problems. We performed simulations for the space dimension ranging from 3 to 5 to establish the universality of the passive scalar statistical behavior in 2d and to reveal features characteristic of higher dimensions. We used a scheme with permanent injection of particles near the wall, which produces a passive scalar statistically homogeneous in time. But our conclusions are also valid for the decaying case because of the adiabaticity: events responsible for the passive scalar transport to the bulk occur much faster than the average passive scalar decay.

The obtained numerical data can be used to compute averages characterizing the passive scalar statistics. First of all, we found moments of the passive scalar at different separations from the wall. The data show the existence of a well-pronounced diffusive layer where the passive scalar is mainly concentrated, in accordance with the theoretical expectations formulated in [22]. Outside the diffusive layer, the passive scalar moments demonstrate scaling behavior with the exponents deviating from those proposed in [22], where the diffusion was assumed to be negligible outside the diffusive layer. We verified that the deviations are indeed related to diffusion. The situation resembles the passive scalar statistics in the Batchelor velocity field on scales larger than the pumping length where diffusion appears to be relevant [24], which corrects the diffusionless behavior examined in [25]. Next, we introduced the passive scalar integrated along a surface parallel to the wall. The diffusion along the wall drops out from the equation for the object. We demonstrated numerically that as functions of the separation from the wall, the moments of the integral passive scalar have a well-pronounced scaling behavior outside the diffusive layer. We found the corresponding scaling exponents for the moments with degrees $n = 1-6$ in space dimension $d = 2-5$. The moments exhibit an anomalous scaling signalling a strong intermittency of the passive scalar statistics.

The simulations enabled us to reveal objects underlying the intermittency. These are tongues of the passive scalar pulled from the diffusive layer towards the bulk. The tongue cross section diminishes as the separation from the wall increases (because the velocity component perpendicular to the wall increases). That explains why diffusion can play an essential role even in the region outside the diffusive layer. The subsequent tongue evolution, including tongue folds, produces long-lived structures of complex shape. Sometimes, the tongues are pulled so strongly that they irreversibly push a passive scalar portion away from the wall. Just this mechanism is responsible for the passive scalar transport to the bulk, which naturally explains its strong intermittency.

As an explanation of the passive scalar statistics, we suggest a theoretical scheme based on the smallness of the passive scalar correlation length along the wall outside the diffusive layer. This scheme allows finding explicit expressions for the scaling exponents characterizing different objects. A comparison of the theoretical predictions with numerical results shows that they agree satisfactorily. Some preliminary results of our work were published in [26].

The structure of this paper is as follows. In Section 2, we present our theoretical approach to the passive scalar dynamics and statistics in the peripheral region and propose a scheme yielding the scaling exponents. In Section 3, we explain our computational scheme, present computed moments of the passive scalar and integral passive scalar, describe the passive scalar tongues, and compare our numerical results with theory. In Conclusion, we summarize our results and discuss their possible applications and directions of future investigations.

2. THEORETICAL DESCIPTION

We consider the passive scalar statistics in peripheral regions of a random flow, i.e., regions near boundaries (walls). Our principal example is the viscous (laminar) boundary layer of the developed high-Reynolds hydrodynamic turbulence (see, e.g., book [8]), but our approach can also be applied to other situations. For example, we can consider the peripheral region of elastic turbulence [12]. The only feature relevant for us is the smoothness of the flow in the boundary layer, whereas the velocity varies randomly in time there.

We let θ denote the passive scalar field. It can represent both temperature variations or the concentration of pollutants. The passive scalar evolution (decay) in an external flow is described by the advection–diffusion equation

$$\partial_t \theta + \mathbf{v}\nabla\theta = \kappa\nabla^2\theta, \qquad (1)$$

where $\mathbf{v}$ is the flow velocity and κ is the diffusion (thermodiffusion) coefficient. Below, the fluid is assumed to be incompressible (that is, the flow is divergenceless, $\nabla\mathbf{v} = 0$). Equation (1) implies that there are no sources of the passive scalar in the bulk. However, we do not exclude a passive scalar flux from the vessel walls.

Equation (1) has to be supplemented by boundary conditions at the wall. If θ is the density of pollutants and the wall is impenetrable for the pollutants, then the gradient of θ in the direction perpendicular to the

wall is zero near the wall, which corresponds to zero pollutant flux to the boundary. In this case, we deal with the passive scalar decay, leading ultimately to its homogeneous distribution in space. If θ is the temperature, then its gradient in the direction perpendicular to the wall can be nonzero, which corresponds to a finite heat flux through the boundary (from the wall). If the walls are made of a material that conducts heat well, then the value of θ (temperature) has to be regarded as fixed at the boundary.

We assume that the Peclet or Schmidt number is large (that is, the diffusion coefficient κ is small in comparison with the fluid kinematic viscosity ν). Then, as was demonstrated in [22], the passive scalar dynamics in the peripheral region is slow in comparison with the velocity dynamics. Therefore, the passive scalar is rapidly mixed in the bulk (for a time that can be estimated as the inverse Lyapunov exponent of the flow), which leads to a homogeneous spacial distribution of the passive scalar, θ = const. The subsequent passive scalar evolution is related mainly to the peripheral regions, which supply the bulk by passive scalar fluctuations. We assume that the bulk can be treated as a big reservoir; then the bulk homogeneous value of θ, θ_b, can be assumed to be independent of time. Below, we assume that the passive scalar field is shifted by θ_b, which leads to the condition $\theta \longrightarrow 0$ as we pass from the periphery to the bulk.

2.1. Correlation Functions

Statistical properties of the passive scalar can be described in terms of its correlation functions

$$F_n(t, \mathbf{r}_1, ..., \mathbf{r}_n) = \langle \theta(t, \mathbf{r}_1)...\theta(t, \mathbf{r}_n) \rangle, \quad (2)$$

where the angular brackets denote averaging over large times (larger than the velocity correlation time). Because the velocity tends to zero in approaching the wall and the molecular diffusion is assumed to be weak, the passive scalar dynamics, determined by an interplay of the advection and diffusion, is slower than the velocity dynamics in the peripheral region. Therefore, in investigating the passive scalar dynamics, the velocity can be regarded as short-correlated in time, and closed equations can be derived for the passive scalar correlation functions (see, e.g., [18, 22])

$$\partial_t F_n = \kappa \sum_{m=1}^{n} \nabla_m^2 F_n$$

$$+ \sum_{m,k=1}^{n} \sum_{\alpha\beta} \partial_{m\alpha}[D_{\alpha\beta}(\mathbf{r}_m, \mathbf{r}_k)\partial_{k\beta}F_n], \quad (3)$$

where $D_{\alpha\beta}$ is expressed in terms of the pair velocity correlation function as

$$D_{\alpha\beta}(\mathbf{r}_1, \mathbf{r}_2) = \int_0^\infty dt' \langle v_\alpha(t+t', \mathbf{r}_1) v_\beta(0, \mathbf{r}_2) \rangle. \quad (4)$$

Here, again, the angular brackets denote averaging over times larger than the velocity correlation time.

The structure of Eq. (3) is quite transparent: the evolution of the passive scalar correlation functions is determined by the molecular diffusion (the first term in the right-hand side) and by the eddy diffusion (the second term in the right-hand side). Therefore, the quantity $D_{\alpha\beta}$ can be called the eddy diffusion tensor, since it describes diffusion of the passive scalar related to the random flow. This effect can be compared to the turbulent diffusion of the passive scalar in turbulent flows in the bulk on scales larger than the viscous length. But in our case, the eddy diffusion tensor $D_{\alpha\beta}$ is associated with a smooth flow, and can be used to describe the passive scalar dynamics on scales smaller than the turbulent viscous length.

We assume that the walls of the vessel are smooth and that the boundary layer width is much less than the curvature radii of the wall. Then it can be treated as flat in the leading approximation. We introduce a reference system with the z axis perpendicular to the wall and assume that the fluid occupies the region $z > 0$. The smoothness of the velocity leads to the proportionality laws v_x, $v_y \propto z$ and $v_z \propto z^2$ for the velocity components along and perpendicular to the wall. The laws are consequences of the velocity smoothness, of the nonslipping boundary condition $\mathbf{v} = 0$ at the wall, and of the incompressibility condition $\nabla \mathbf{v} = 0$.

Below, we assume that the velocity statistics is homogenous in time, and also assume its homogeneity along the wall. Due to the assumed homogeneity, velocity correlation functions depend on time differences and on the differences of the coordinates x and y. For example, eddy diffusion tensor (4) is independent of time and does depend on the differences $x_1 - x_2$ and $y_1 - y_2$. However, it depends on both z_1 and z_2 due to the strong inhomogeneity of the system in the direction perpendicular to the wall. The z-dependence of the eddy diffusion tensor components can be found directly from the proportionality laws v_x, $v_y \propto z$ and $v_z \propto z^2$. For example,

$$D_{zz}(x, y, z_1; x, y, z_2) = \mu z_1^2 z_2^2, \quad (5)$$

where μ is a constant characterizing the strength of the velocity fluctuations in the peripheral region.

The equation for the first moment of θ (the average value of the passive scalar field), $\langle \theta \rangle$, is

$$\partial_t \langle \theta \rangle = \partial_z[\mu z^4 \partial_z \langle \theta \rangle] + \kappa \partial_z^2 \langle \theta \rangle, \quad (6)$$

as follows from Eqs. (3) and (5). Comparing the advection and the diffusion terms in Eq. (6), we finds a characteristic diffusion length r_{bl} defined as

$$r_{bl} = (\kappa/\mu)^{1/4}. \quad (7)$$

This quantity determines the thickness of the diffusion boundary layer formed near the wall. Due to the smallness of κ (we recall that the Peclet or the Schmidt number is assumed to be large), the diffusion length is

much less than the thickness of the peripheral region, where the law $v_z \propto z^2$ holds.

We consider an advanced stage of the passive scalar decay or a statistically stationary situation caused by a permanent passive scalar flux through the wall. Then the passive scalar θ is nonzero primarily in the diffusive boundary layer, at $z \lesssim r_{bl}$. We recall that we shifted the field $\theta \longrightarrow \theta - \theta_b$, where θ_b is its value in bulk. After the shift the field θ could be positive or negative (depending on boundary conditions) and should tend to zero in the bulk, that is, as $z \longrightarrow \infty$. But we are mainly interested in the passive scalar transport through the region $z \gg r_{bl}$, where the passive scalar is carrying from the diffusive boundary layer to the bulk. There, we may neglect the molecular diffusion term in Eq. (6), which yields the proportionality law

$$\langle \theta \rangle \propto z^{-3}. \qquad (8)$$

This gives the decay rate of $\langle \theta \rangle$ as z increases. We note that the law in (8) corresponds to a constant average passive scalar flow through the planes $z = $ const, that is, the flux is independent of z.

It can be anticipated that at $z \gg r_{bl}$, the higher passive scalar moments have some scaling behavior as $\langle \theta \rangle$ has. We introduce the corresponding scaling exponents

$$\langle \theta^n \rangle \propto z^{-\eta_n}. \qquad (9)$$

If the molecular diffusion is irrelevant outside the diffusion boundary layer, then $\eta_n = 3$ [22]. However, our numerical data imply that the molecular diffusion is relevant even at $z \gg r_{bl}$ (we give an explanation of this phenomenon in what follows). Therefore, the exponents η_n are not equal to 3 and their values are a subject of special investigation.

We turn to passive scalar correlation functions (2). At $z \gg r_{bl}$, their dependence on the coordinates along the wall are characterized by a correlation length l that can be found from the balance of the molecular and the eddy diffusion along the wall. The eddy diffusivity term in Eq. (3) can be estimated as μz^2 (see Eq. (5); the z^2 law follows from the z-dependence of the velocity components). Comparing the molecular diffusion term $\sim \kappa/l^2$ and the eddy diffusion term in Eq. (3), we find

$$l \sim \sqrt{\kappa/\mu} z^{-1}. \qquad (10)$$

The quantity is of the order of r_{bl} at $z \sim r_{bl}$ and decreases as z^{-1} as z increases.

2.2. Integral Passive Scalar

To exclude the effects of molecular diffusion, we introduce an integral of the passive scalar field along a surface parallel to the wall,

$$\Theta(t, z) = A^{-1} \int dx dy \theta(t, x, y, z), \qquad (11)$$

where A is the area of the surface and z is its separation from the wall. We let

$$\Phi_n(t, z_1, ..., z_n) = \langle \Theta(t, z_1) ... \Theta(t, z_n) \rangle \qquad (12)$$

denote the corresponding correlation functions. Integrating Eq. (3) over x_k and y_k, we obtain

$$\partial_t \Phi_n = \kappa \sum_{m=1}^{n} \partial_{mz}^2 \Phi_n + \int dx_1 ... dx_n dy_1 ... dy_n$$

$$\times \left\{ \sum_{m,k=1}^{n} \partial_{mz} [D_{zz} \partial_{kz} F_n] \right. \qquad (13)$$

$$\left. + \sum_{m \neq k} \partial_{mz} [(\partial_{kz} D_{zz}) F_n] \right\},$$

where $D_{zz} = D_{zz}(\mathbf{r}_m, \mathbf{r}_k)$. In deriving Eq. (13), we took some integrals by part and used the constraint

$$\frac{\partial}{\partial x_k} D_{xx}(\mathbf{r}_m, \mathbf{r}_k) + \frac{\partial}{\partial y_k} D_{zy}(\mathbf{r}_m, \mathbf{r}_k)$$

$$+ \frac{\partial}{\partial z_k} D_{zz}(\mathbf{r}_m, \mathbf{r}_k) = 0,$$

which is a consequence of the incompressibility condition $\nabla \mathbf{v} = 0$.

We expect a scaling behavior of correlation functions (12) at $z \gg r_{bl}$. Then the last term in Eq. (13) can be estimated as $\mu z^4 \partial_z^2 \Phi$. Consequently, the term with the molecular diffusion κ, in Eq. (13) can be neglected in the region. The argument is the same as the one used for the moment $\langle \theta \rangle$, where the law (8) was derived from Eq. (6). We also note that in the decaying case, the time derivative in Eq. (13) can be estimated as $\kappa/r_{bl}^2 = \sqrt{\kappa \mu}$, a term that is much less than $\mu z^4 \partial_z^2 \sim \mu z^2$ at $z \gg r_{bl}$. Therefore, the term with the time derivative can be neglected in the region as well, and we obtain quasistationary equations for Φ_n. This reflects the adiabaticity of the passive scalar statistics.

It is reasonable to assume that the correlation function $F_n(t, \mathbf{r}_1, ..., \mathbf{r}_n)$ is correlated along the xy plane on distances of the order of the correlation length l in (10), which is much smaller than the characteristic velocity length (the width of the peripheral region). Then D_{zz} in Eq. (13) can be replaced by $\mu z_m^2 z_k^2$, and we obtain closed equations for the correlation functions

$$\partial_t \Phi_n(t, z_1, ..., z_n) = \mu \sum_{m,k=1}^{n} \frac{\partial}{\partial z_m} \left(z_m^2 z_k^2 \frac{\partial}{\partial z_k} \Phi_n \right)$$

$$+ 2\mu \sum_{m \neq k} \frac{\partial}{\partial z_m} (z_m^2 z_k \Phi_n), \qquad (14)$$

where we omitted the molecular diffusion term (see the above argumentation).
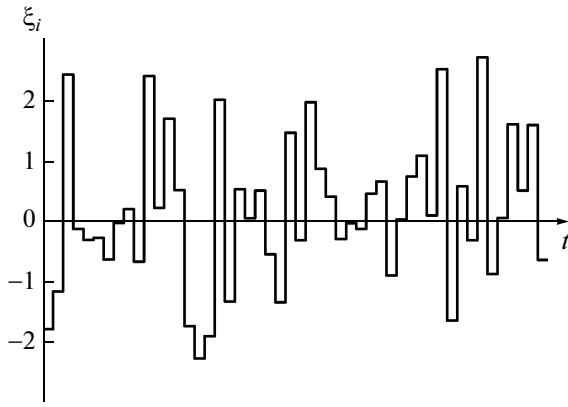
Fig. 1. An example of the telegraph process.

Equations (14) lead to the following closed equations for the moments of the integral passive scalar:

$$\partial_t \langle \Theta^n \rangle = \mu [z^4 \partial_z^2 + 4n z^3 \partial_z + 4n(n-1)z^2] \langle \Theta^n \rangle. \quad (15)$$

In the stationary (or quasistationary) case (where $\partial_t \langle \Theta^n \rangle$ is negligible), we obtain a homogeneous differential equation for the nth moment, which admits a power solution

$$\langle \Theta^n \rangle \propto z^{-\zeta_n}. \quad (16)$$

The exponents ζ_n can be easily found from Eq. (15) as

$$\zeta_n = 2n - 1/2 + \sqrt{2n + 1/4}. \quad (17)$$

We have chosen the positive sign of the square root leading to the reference value $\zeta_1 = 3$, as it should be in accordance with Eq. (8). We observe an anomalous scaling, that is, a nonlinear dependence of ζ_n on n, which can be compared to the anomalous scaling of the passive scalar in the Kraichnan model [14−16].

A natural conjecture that allows relating the moments of the passive scalar θ and those of the integral passive scalar Θ is that the passive scalar correlation length l can be used as a recalculation factor. We then obtain the estimate

$$\langle \Theta^n \rangle \sim \frac{l^{(d-1)(n-1)}}{A^{n-1}} \langle \theta^n \rangle, \quad (18)$$

where d is the space dimension, which is equal to 3 in real flows but can be arbitrary in numerical simulations. Estimate (18) and Eq. (10) lead to the relation

$$\eta_n = \zeta_n - (n-1)(d-1), \quad (19)$$

between the exponents introduced in Eqs. (9) and (16).

3. SIMULATIONS

We conducted Lagrangian simulations where the dynamics of a large number of particles subjected to flow advection and Langevin forces (producing diffusion) was examined. A set of particles was used instead of the passive scalar field θ, which can be interpreted as the density of the particles. A major advantage of our approach is its applicability to different space dimensions d. Indeed, the number of variables (coordinates of particles) in the scheme grows not exponentially but as a power of d (at a fixed number of the particles).

To establish principal qualitative features of the passive scalar transport, we mainly performed $2d$ simulations. The setup is periodic in x (the coordinate along the wall) with a period L. In the majority of simulations, the velocity field was chosen to be

$$v_x = z \Big(\xi_1 \cos \frac{2\pi x}{L} + \xi_2 \sin \frac{2\pi x}{L} \Big) \frac{L}{\pi}, \quad (20)$$

$$v_z = z^2 \Big(\xi_1 \sin \frac{2\pi x}{L} - \xi_2 \cos \frac{2\pi x}{L} \Big), \quad (21)$$

where ξ_1 and ξ_2 are independent random functions of time. We emphasize that the velocity field in (20) and (21) satisfies the incompressibility condition $\partial_x v_x + \partial_z v_z = 0$ for any functions $\xi_1(t)$ and $\xi_2(t)$. If these are chosen to have identical Gaussian probability distributions, then the statistics of velocity field (20) and (21) is homogeneous in x (along the wall). In our simulations, we have chosen $L = 10$.

In reality, the proportionality laws $v_x \propto z$ and $v_x \propto z^2$ are satisfied inside the laminar boundary layer, but in our setup, the expressions for the velocity components like (20) and (21) are formally used at all z, which means that the bulk corresponds to $z = \infty$. However, the law $v_z \propto z^2$ implies that the particles may reach the z-infinity in a finite time. This ensures a finite particle flux to the bulk since a finite number of particles sometimes pass there. Hence, the passive scalar transport to the bulk is well defined in our setup.

Because the velocity correlation time in the peripheral region is much less than the passive scalar mixing time, we should regard $\xi_1(t)$ and $\xi_2(t)$ as white noises. But zero correlation time cannot be realized in computer simulations. We model the functions by telegraph processes, where both ξ_1 and ξ_2 remain constants inside time slots of a small duration τ, and the values of ξ_1 and ξ_2 inside the slots are chosen to be random variables with identical normal distributions. An example of such a telegraph process is plotted in Fig. 1. In our simulations, the averages were $\langle \xi_1^2 \rangle = \langle \xi_2^2 \rangle = 1$ and different slot sizes were used, $\tau = 0.001$, 0.002, and 0.004. Then, in accordance with definition (5), $\mu = \tau/2$.

In our scheme, a particle trajectory $\rho(t)$ obeys the equation

$$\partial_t \rho = v(t, \rho) + \zeta(t), \quad (22)$$

where the first term represents the particle advection and the second term represents the Langevin force. We emphasize that the variables ζ pertaining to different

particles are independent, whereas the variables ξ_1 and ξ_2 are identical for all particles, according to the physical meaning of the variables. The Langevin force ζ is also modeled by a telegraph process with the same time slot duration τ and with normal distributions of the values in the slots. To ensure a given value of the diffusion coefficient κ, we choose

$$\langle \zeta_x^2 \rangle = \langle \zeta_z^2 \rangle = 2\kappa/\tau. \qquad (23)$$

In a majority of simulations, we chose $\kappa = \tau/2$, and therefore the diffusive length was $r_{bl} = 1$, in accordance with definition (7).

Inside a time slot, all the variables ξ_1, ξ_2, and ζ are time-independent constants and Eq. (22) becomes an autonomous ordinary differential equation. It was solved as follows. A time slot was divided into a number of time intervals and the equation was solved (without the Langevin force) using the second-order Runge–Kutta method. The number of intervals is z-dependent, being proportional to z at $z > 2.5$. For $z > 12$, we solved equations for $1/\rho_z$ instead of ρ_z. Both features are motivated by the strong dependence of the velocity on z, $v_z \propto z^2$. After solving the equation inside a slot, a term produced by the Langevin force was added. To examine the role of diffusion outside the diffusive boundary layer, we switched off the diffusion (the Langevin forces) in some simulations at distances $z > z_d$ (with z_d chosen differently in different cases).

The particles are permanently injected near the wall in random positions at the beginning of each time slot. The simulations were performed in the stripe $0 < z < 100$; the particles crossing the lines $z = 0$ and $z = 100$ were excluded from the set. The number of particles leaving the region $0 < z < 100$ through the wall is much larger than the number of particles escaping through the line $z = 100$. Those last ones correspond to the passive scalar transport to the bulk. A balance between the particle injection and losses leads to a statistical equilibrium achieved gradually in the simulation. Hence, our simulations cover the statistically stationary passive scalar transport. It corresponds both to a steady temperature distribution supported by a constant heat flux from the wall and to a decay of the concentration of pollutants that can be treated adiabatically.

An extension of our scheme to higher dimensions, $d > 2$, is straightforward. We use the same Eq. (22) where all quantities have d components. The Langevin forces ζ are determined by the same relations (23) and a generalization of expressions (20) and (21) is as follows. The velocity $\mathbf{v}$ is determined by a set of $2(d-1)^2$ random variables ξ_{1ij} and ξ_{2ij}:

$$v_i = z \sum_{j=1}^{n-1} \left(\xi_{1ij} \cos \frac{2\pi x_j}{L} + \xi_{2ij} \sin \frac{2\pi x_j}{L} \right) \frac{L}{\pi}, \qquad (24)$$

$$v_z = z^2 \sum_{j=1}^{n-1} \left(\xi_{1jj} \sin \frac{2\pi x_j}{L} - \xi_{2jj} \cos \frac{2\pi x_j}{L} \right), \qquad (25)$$

where the subscripts i, j label the first $d - 1$ space coordinates and the last dth coordinate is z. Here, all ζ, ξ_{1ij}, and ξ_{2ij} are again telegraph processes with the same statistical properties as above, and we use the second-order Runge–Kutta scheme inside a time slot.

In terms of the particles, the passive scalar field θ is defined as the number of particles per unit volume. The correspondence is correct if θ is positive. If θ is negative, then the particle density represents $-\theta$, which satisfies the same Eq. (1) as θ does. Thus, in our simulations, we should treat θ as the number of particles inside a box divided by the box volume. Of course, the definition works well if the box is small (in comparison with all characteristic scales of the problem) and the number of particles inside the box is large. To satisfy these contradictory conditions, we must deal with a sufficiently large total number of particles. That is why the injection rate in our simulations is chosen to produce a large number of particles, 10^5–10^6, in statistical equilibrium.

3.1. Tongues

Our simulations show that the passive scalar transport to the bulk is related to specific structures of the passive scalar. The passive scalar is concentrated mainly in the narrow diffusive layer near the wall. However, a fluid jet is sometimes generated that carries the passive scalar from the wall towards the bulk and produces a passive scalar tongue with the width (cross section) decreasing as z increases. This property is a consequence of the law $v_z \propto z^2$ implying that the z-component of the tongue velocity increases as z increases. We thus come to a geometric interpretation of the passive scalar correlation length l: it is the characteristic size of the tongue cross section (taken along the wall). The cross section behavior corresponds to the expected decrease of the correlation length as z increases. We stress that in accordance with Eq. (10), the characteristic tongue cross section depends on the diffusion coefficient κ.

A tongue is typically pulled from a "bump" of the passive scalar distribution. After some time, the tongue is tilted and then pressed back to the diffusive layer. Then next tongue is pulled, usually from the bump remaining at the bottom of the previous tongue, and is in turn pressed back to the diffusive layer. As a result, a complicated multifold structure is formed, an example of which is shown in Fig. 2, which represents a snapshot generated in our simulations.

Sometimes the tongue is pulled up to the z-infinity, and then a portion of the passive scalar (a number of particles) is pushed to the bulk. After that, the tongue is tilted and the passive scalar current to the bulk stops. This implies that the passive scalar flux, $\int dx \theta v_z$ in $2d$, is a highly intermittent quantity at $z > r_{bl}$. This conclusion is confirmed by the flux histograms drawn in Fig. 3 for different z. In the simulations, the passive
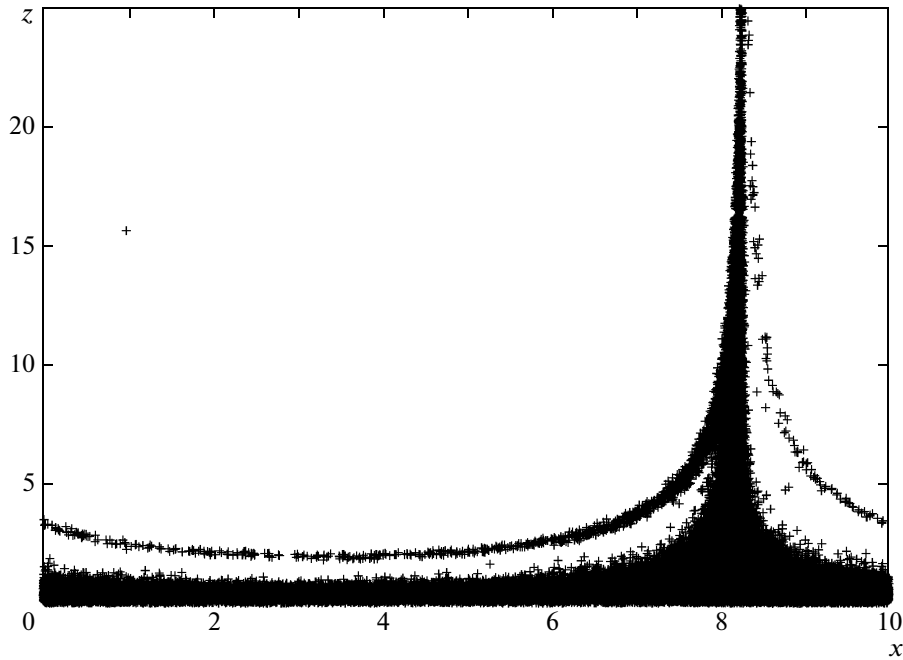
Fig. 2. An example of a passive scalar structure formed near the wall in a 2d random flow. Different particles are designated by small crosses.

scalar flux was measured as the number of particles crossing the plain $z = $ const in a time interval τ. At $z = 0$, the flux probability distribution is practically Gaussian, being formed by a balance between the random injection of the particles and their leaving the wall. But the distribution becomes less and less Gaussian as z increases. The histograms in Fig. 3 are practically symmetric. The property is because only a small amount of particles in the tongue are pulled to the bulk, the majority of the particles returns, producing

practically equal fluxes to the bulk and towards the wall. This explains why the root-mean-square fluctuation of the flux at $z \gg r_{\mathrm{bl}}$ is much larger than its average value.

3.2. Moments

Based on numerical data, we can compute moments and correlation functions of different quantities characterizing the passive scalar statistics. We can consider both local functions and integral objects. All the quantities are computed as time averages.

We introduce an object θ_δ that is the number of particles inside a square box of size δ divided by its area δ^2 (in 2d). The quantity θ_δ is close to θ if the number of particles is large and the size of the box is sufficiently small. The moments $M_n = \langle \theta_\delta^n \rangle$ of θ_δ are computed for $n = 1-6$ as averages over time intervals $10^6-10^7\tau$ with $\delta = 0.03125$. The results are presented in Fig. 4, where the moments multiplied by z^3 are plotted in log–log coordinates (solid curves). We see that the prediction for the first moment in (8) is perfectly supported, whereas higher moments deviate strongly from the diffusionless law $\propto z^{-3}$. We conclude that the diffusion is indeed relevant at $z > r_{\mathrm{bl}}$.
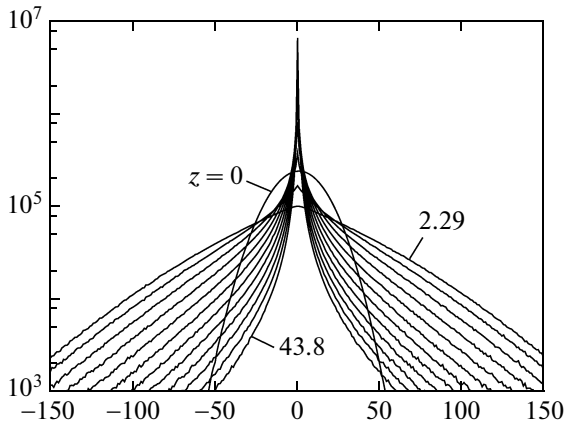

Fig. 3. Histograms of the passive scalar flux at different separations from the wall. The root-mean-square fluctuations are much larger than the average value and the histograms are practically symmetric. At $z = 0$, the probability distribution is Gaussian, whereas at $z > r_{\mathrm{bl}}$, it has exponential tails.

To verify this conclusion, we repeated the simulations switching the diffusion off at $z > 3$ and at $z > 12$. The results are shown in Fig. 4 with dashed curves. We see the appearance of plateaus, starting just from $z = 3$ or $z = 12$ and corresponding to the law $\propto z^{-3}$, in accor-
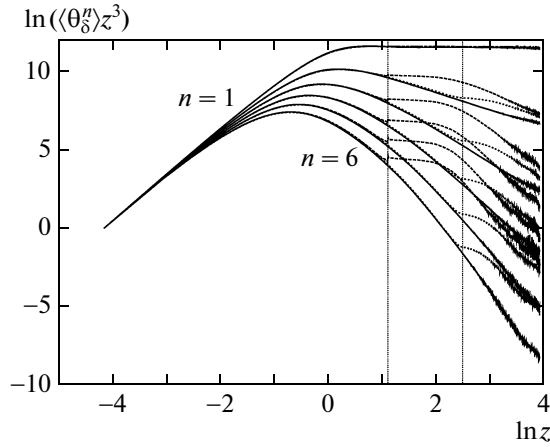
Fig. 4. Log–log plot of the moments $\langle \theta_\delta^n \rangle$ times z^3, for $\delta = 0.03125$ and $n = 1$–6. The graph reflects simulations where diffusion occurs everywhere, and is switched off at $z = 3$ or $z = 12$.
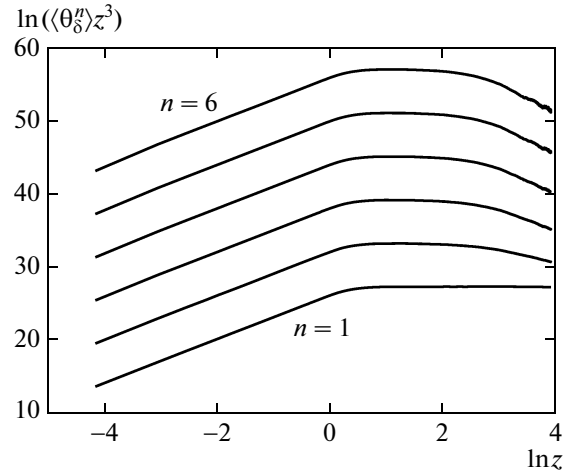

Fig. 5. Log–log plot of the moments $\langle \theta_\delta^n \rangle$ times z^3, for $\delta = 0.03125$ and $n = 1$–6 in the case where diffusion is substituted by a constant velocity carrying the particles away from the wall.

dance with [22]. The plateaus are observed in restricted regions of separations from the wall z, slightly diminishing as n increases. An explanation is that cutoffs of the plateaus are observed where δ becomes of the order of the passive scalar correlation length (along the wall). To check this, we repeated the simulations for larger values of δ and observed that the plateaus shrink as δ increases. This confirms our explanation. To be absolutely sure that the diffusion is relevant, we performed simulations without diffusion but with a constant velocity V added that carries the particles away from the wall. The results are presented in Fig. 5, where the moments $\langle \theta_\delta^n \rangle$ times z^3 are plotted. We see the plateaus signalling that outside the boundary layer, the passive scalar moments behave in accordance with the diffusionless prediction.

The next object of our investigation is the integral quantity Θ that is the passive scalar integrated along the wall (see definition (11)). Numerically, it is determined by the number of particles in a slice of thickness δ, parallel to the wall, divided by its volume (area); we let the ratio be denoted by Θ_δ. In our $2d$ setup, the area is equal to $L\delta$, where δ is chosen to be much less than z. The moments $\langle \Theta_\delta^n \rangle$ are computed by time averaging over a long time $\sim 10^7\tau$. To check the robustness of the results, we performed computations for different time slots $\tau = 0.001$, 0.002, and 0.004 and for four different values of the diffusion coefficient κ. Figure 6 demonstrates that the values of each moment collapse to a single curve in the logarithmic coordinates $\ln(z/r_{bl})$ and $\ln(\langle \Theta^n \rangle /C_n)$, where the factors C_n are the corresponding moments near the wall.

It can be verified that in accordance with our theoretical expectations, the moments of Θ_δ are insensitive

to diffusion. In Fig. 7, to illustrate this assertion, we present the moments of Θ_δ computed at $\tau = 0.002$ in two cases: in the first case, the diffusion occurs everywhere and in the second case, it is switched off at $z > 3$. We can observe no difference between the data. An alternative to the velocity field in (20), (21) can also be used. In Fig. 7, we plot two sets of data: those corresponding to velocity (20), (21) and to the velocity with four random factors

$$\frac{\pi v_x}{Lz} = \xi_1 \cos\frac{2\pi x}{L} + \xi_2 \sin\frac{2\pi x}{L} + \xi_3 \cos\frac{4\pi x}{L} + \xi_4 \sin\frac{4\pi x}{L}, \tag{26}$$
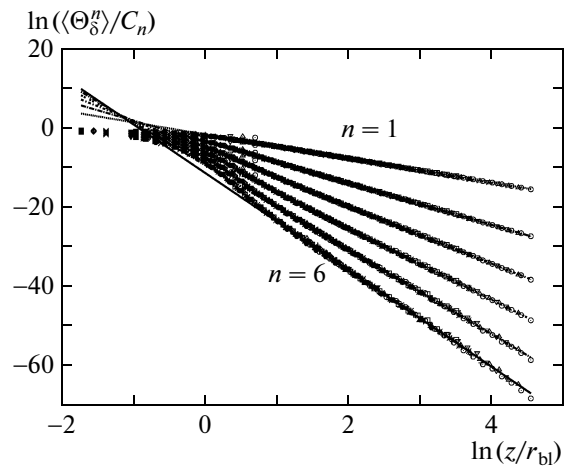

Fig. 6. Moments of Θ_d in log–log coordinates, $n = 1$–6. In the region $z > r_{bl}$, the results collapse onto single curves for three times $\tau = 0.001$, 0.002, and 0.004 and four different values of the diffusion coefficient.
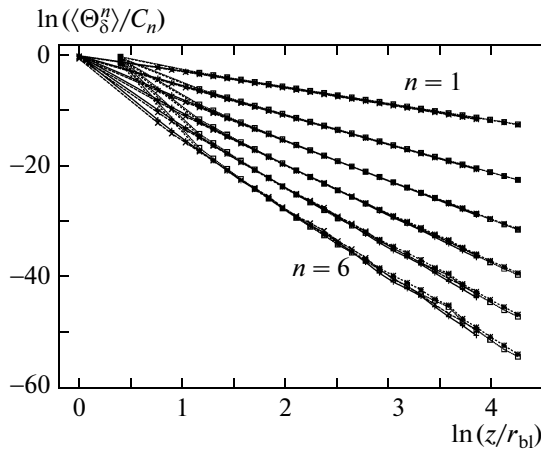
Fig. 7. Moments of Θ_d in logarithmic coordinates, $n = 1-6$. The results are obtained for two cases where the diffusion occurs everywhere and where it is switched off at $z > 3$, and also for two different velocity fields: with two and four harmonics.

$$\frac{v_z}{z^2} = \xi_1 \sin\frac{2\pi x}{L} - \xi_2 \cos\frac{2\pi x}{L}$$
$$+ 2\xi_3 \sin\frac{4\pi x}{L} - 2\xi_4 \cos\frac{4\pi x}{L}. \tag{27}$$

Again, there is no visible difference between these sets of data.

We observe that the moments of Θ are decreasing functions of z that are power-like in the region $z > r_{bl}$. Extracting the scaling exponents ζ_n (see definition (17)) for $n = 1-6$ in $2d$, we obtain values that are prese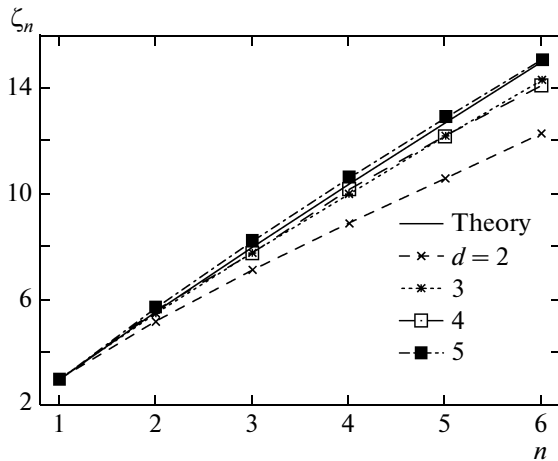nted in Fig. 8 as the lower set of points (a smooth curve is drawn through the points to guide the eye). We conducted analogous simulations for higher dimensions, up to $d = 5$. The results are also depicted in Fig. 8. We see that the exponents ζ_n depend on d, but for $d \geq 3$, they are close to theoretical values (17) represented by a solid line.

It can be assumed that the deviations from theoretical values (17) are related to the existence of additional passive scalar (relatively long) correlations along the wall that can be produced by the multifold structures of the type shown in Fig. 2. The long correlations should lead to increasing moments of the passive scalar in comparison with the short-correlated case. It is natural to expect that the fold effect becomes less pronounced in higher dimensions. Indeed, Fig. 8 shows that the deviations from the values in (17) decrease as the space dimensionality d increases. This confirms our explanation.

To check our conjecture, we conducted simulations for the velocity field, similar to expressions (26) and (27), containing a set of harmonics in terms of the period L: the 9th, 10th, and 11th ones. In such a velocity field, correlations related to the multifold tongue structures must be suppressed, and, consequently, the exponents ζ_n must be close to theoretical values (17). This expectation is confirmed by our simulations; the results are presented in Fig. 9, where the measured exponents are plotted. We see a good agreement of the measured and theoretical exponents.

The exponents η_n of the moments of θ_δ, see definition (9), as well as ζ_n, can be extracted from our numerical data. It is interesting to check theoretical prediction (19). For this, we plotted the difference $\zeta_n - \eta_n$ as a function of n (see Fig. 10). For compari-
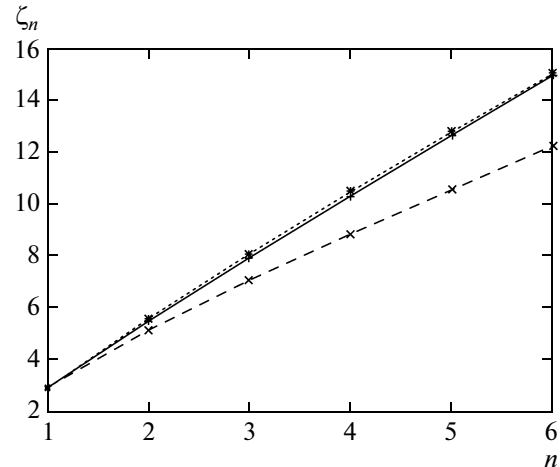

Fig. 8. Exponents of the moments $\langle \Theta_\delta^n \rangle$, for $n = 1-6$ and space dimensions $d = 2-5$. For comparison, the theoretical curve $\zeta_n = 2n - 1/2 + \sqrt{2n + 1/4}$ is plotted (solid line).

Fig. 9. Exponents of the moments $\langle \Theta_\delta^n \rangle$, for $n = 1-6$ and space dimension $d = 2$ for two different velocity fields: containing only the first harmonic (dashed line) and three (9th, 10th, and 11th) harmonics (dotted line). For comparison, the theoretical curve $\zeta_n = 2n - 1/2 + \sqrt{2n + 1/4}$ is plotted (solid line).
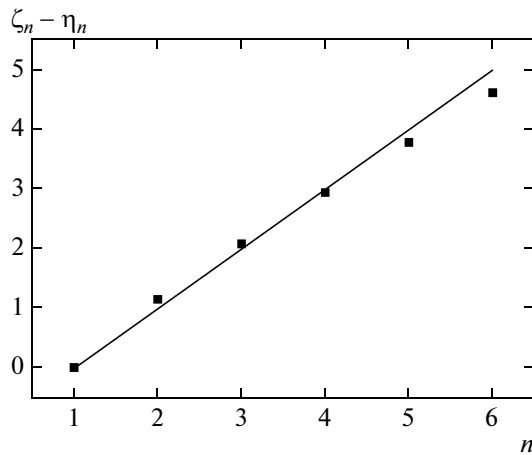
Fig. 10. The difference of the scaling exponents of moments for the integral passive scalar and for the passive scalar, $\zeta_n - \eta_n$, computed at $\delta = 0.03125$ in $2d$. For comparison, the theoretical prediction $n - 1$ is drawn.

son, the theoretical straight line $n - 1$ (correct in $2d$) is drawn in the same figure. We see a good agreement, confirming the scaling (10) of the passive scalar correlation length $l(z)$ along the wall.

4. CONCLUSIONS

We performed extensive numerical simulations of the passive scalar mixing in peripheral regions of random flows such as high-Reynolds turbulence. The simulations confirm earlier theoretical expectations and reveal numerous new details. At advanced stages of the passive scalar mixing, passive scalar fluctuations are concentrated mainly in a narrow diffusive layer near the boundary if the Peclet or the Schmidt number is large. We found that the passive scalar transport from the diffusive boundary layer to the bulk is related to passive scalar tongues formed by jets directed to the bulk. The tongues are objects responsible for the strong intermittency characteristic of the passive scalar transport through the peripheral region.

We examined the passive scalar statistics outside the diffusive boundary layer and realized that the moments of both the passive scalar θ and the passive scalar integrated along the wall, Θ, exhibit well-pronounced scaling in terms of the separation from the wall z. We compared the corresponding exponents extracted from our simulations with our theoretical scheme and established their agreement. However, care must be taken because our theoretical predictions are correct for an infinite vessel and can be violated in simulations where the velocity correlation length along the wall coincides with the velocity period. We also found an agreement between the theoretical prediction for the tongue cross section dependence on z and our simulations. Therefore, the simulations confirm our theoretical predictions.

There remain some problems to be solved in future. We will extend our consideration to incorporate average flows (like in pipes) that are shear-like near the wall. Another natural extension of our approach is related to chemical reactions in random flows. We also note polymer solutions, where the polymer elongation is very sensitive to the character of the flow. The problem is significant, e.g., for the elastic turbulence. However, a long-time memory characteristic of the polymer solutions could modify our results. We considered smooth walls in our work. There is a set of questions related to the wall roughness, possible corners, caverns and peaks. All these may modify our conclusions, and this is a subject of special investigation.

Our results agree qualitatively with the data known from investigations of turbulent plumes in turbulent flows, where a complicated space structure of the passive scalar fluctuations is observed [27–31]. We believe that statistical properties of the structure can be explained on the basis of our results implying production of the passive scalar tongues pushing to the bulk. The explanation requires generalizing our scheme to the case where turbulent velocity fluctuations in the bulk are included.

REFERENCES

1. A. M. Obukhov, Izv. Akad. Nauk. SSSR, Ser. Geogr. Geofiz. **13**, 58 (1949).

2. S. Corrsin, J. Appl. Phys. **22**, 469 (1951).

3. A. N. Kolmogorov, Dokl. Akad. Nauk SSSR **32**, 16 (1941).

4. K. R. Sreenivasan, Phys. Fluids **8**, 189 (1996).

5. Z. Warhaft, Annu. Rev. Fluid Mech. **32**, 203240 (2000).

6. J. Schumacher and K. R. Sreenivasan, Phys. Fluids **17**, 125107 (2005).

7. R. J. Miller, L. P. Dasi, and D. R. Webster, Exp. Fluids **44**, 719 (2008).

8. A. S. Monin and A. M. Yaglom, *Statistical Fluid Mechanics* (Massachusetts Institute of Technology Press, Cambridge, Massachusetts, United States, 1975).

9. M. Lesieur, *Turbulence in Fluids* (Kluwer, Dordrecht, The Netherlands, 1997).

10. U. Frisch, *Turbulence: The Legacy of A. N. Kolmogorov* (Cambridge University Press, New York, 1995).

11. J. M. Ottino, *The Kinematics of Mixing: Stretching, Chaos, and Transport* (Cambridge University Press, Cambridge, United Kingdom, 1989).

12. A. Groisman and V. Steinberg, Nature (London) **405**, 53 (2000); A. Groisman and V. Steinberg, Phys. Rev. Lett. **86**, 934 (2001); A. Groisman and V. Steinberg, Nature (London) **410**, 905 (2001).

13. V. Kantsler and V. Steinberg, Phys. Rev. Lett. **95**, 258101 (2005).

14. K. Gawedzki and A. Kupiainen, Phys. Rev. Lett. **75**, 3608 (1995).

15. B. Shraiman and E. Siggia, C. R. Acad. Sci., Ser. II: Mec., Phys., Chim., Sci. Terre Univers **321**, 279 (1995).

16. M. Chertkov, G. Falkovich, I. Kolokolov, and V. Lebedev, Phys. Rev. E: Stat. Phys., Plasmas, Fluids, Relat. Interdiscip. Top. **52**, 4924 (1995).

17. B. I. Shraiman and E. D. Siggia, Nature (London) **405**, 639 (2000).

18. G. Falkovich, K. Gawedzki, and M. Vergassola, Rev. Mod. Phys. **73**, 913 (2001).

19. T. Burghelea, E. Segre, and V. Steinberg, Phys. Fluids **19**, 053104 (2007).

20. M. Chertkov and V. Lebedev, Phys. Rev. Lett. **90**, 034501 (2003).

21. M. Chertkov and V. Lebedev, Phys. Rev. Lett. **90**, 134501 (2003).

22. V. V. Lebedev and K. S. Turitsyn, Phys. Rev. E: Stat., Nonlinear, Soft Matter Phys. **69**, 036301 (2004).

23. T. Burghelea, E. Segre, and V. Steinberg, Phys. Rev. Lett. **92**, 164501 (2004).

24. M. Chertkov, I. Kolokolov, and V. Lebedev, Phys. Fluids **19**, 101703 (2007).

25. E. Balkovsky, G. Falkovich, V. Lebedev, and M. Lysiansky, Phys. Fluids **11**, 2269 (1999).

26. A. Chernykh and V. Lebedev, JETP Lett. **87** (12), 682 (2008).

27. J.-Y. Vincont, S. Simoens, M. Ayrault, and J. M. Wallace, J. Fluid Mech. **424**, 127 (2000).

28. J. P. Crimaldi, M. B. Wiley, and J. R. Koseff, J. Turbul. **3**, 014 (2002).

29. J. P. Crimaldi and J. R. Koseff, J. Fluid Mech. **6**, 573 (2006).

30. J. P. Crimaldi, J. R. Koseff, and S. G. Monismith, Phys. Fluids **18**, 095102 (2006).

31. L. P. Dasi, F. Schuerg, and D. R. Webster, J. Fluid Mech. **588**, 253277 (2007).